ELSEVIER

Journal of Chromatography A, 796 (1998) 195–209

JOURNAL OF CHROMATOGRAPHY A

Preparative gradient elution chromatography of chemotactic peptides

Billy Kim, Ajoy Velayudhan*

Department of Bioresource Engineering, Oregon State University, Corvallis, OR 97331, USA

Abstract

Experimental and computational studies are carried out on the separation of a mixture of chemotactic peptides by reversed-phase gradient elution on commercial octadecyl silica supports with acetonitrile as the modulator. The solubility of this mixture is found to be a complex function not only of mobile phase composition, but also of the order in which the various constituents of the mobile phase are mixed together. In certain cases, the feeds seem to reach a metastable state in which they are fully soluble for several hours: this is exploited here for preparative separations. Separations are also carried out by stepwise and nonlinear isocratic elution, and the yields and productivities compared to those from gradient elution. Predictive simulations of all these separations are run using independently measured single component feed isotherms. Good agreement with experiment is found when multicomponent (nonlinear) feed interactions are accounted for, but not when the usual assumption of linear feed isotherms is made. Simultaneous concentration and separation of these feeds is easily achieved by gradient elution. Simulations indicate that the combination of the focusing power of the gradient with the multicomponent feed interactions is likely to give good separations even at high feed loadings.

Keywords: Preparative chromatography; Gradient elution; Mobile phase composition; Solubility parameters; Adsorption isotherms; Simulation studies

1. Introduction

Gradient elution chromatography is widely used as both an analytical and a preparative technique in the separation and purification of a wide variety of products, ranging from relatively small molecules like amino acids and antibiotics to large molecules like polypeptides and proteins [1–5]. The preparative separation of proteins by ion-exchange chromatography is well described in Yamamoto et al. [4]. Gallant et al. [6] present results for the gradient elution of proteins in ion-exchange. While many papers deal with preparative separations of biological mixtures by reversed-phase chromatography, relatively few compare the experimental results to simulations based on nonlinear multicomponent adsorption isotherms. Antia and Horváth [7] present simulations for binary feeds. El Fallah and Guiochon [8] describe the overloaded gradient elution of lysozyme. El Fallah and Guiochon [9,10] and Jandera et al. [11] compare experiments to simulations for the separation of small organic molecules.

The analysis of preparative gradient elution runs is typically made under two standard assumptions. The first is ‘gradient linearization’ [4,12], where feed isotherms in the presence of the modulator are regarded as effectively linear. The presence of the modulator suppresses the isotherms of the feed components, thereby reducing their curvature and generating a larger region over which they can be considered linear. It will be shown in the present

*Corresponding author.

0021-9673/98/$19.00
PII S0021-9673(97)01142-4

work that this assumption, while physically plausible, fails for highly overloaded gradient runs.

The second standard assumption is constancy of gradient shape, i.e., the gradient schedule fed into the column at the inlet is identical in shape to that at the outlet. This is based on regarding the modulator itself as either linearly retained [7,12,13] or unretained [1–3,14]. However, it has been shown that acetonitrile adsorption can be appreciably nonlinear on polymeric sorbents [15,16]. This leads to gradient deformation — the gradient shape at the column outlet can be quite different from its shape at the inlet — and ultimately to the formation of gradient shock layers. It turns out that acetonitrile adsorbs less strongly on silica-based reversed-phase adsorbents, producing less deformation of the gradient schedule [16]. Nevertheless, the retention of the solutes is changed by about 5–10% (e.g., [10]). The implications for large-scale runs on silica-based sorbents, where the change in feed retention due to gradient sorption is likely to be far greater, will be discussed later in this paper.

The present work describes a systematic study combining theory and experiment on the separation of a mixture of peptides by reversed-phase gradient elution chromatography. These closely related feed components are known to be implicated in bacterial chemotaxis [17,18]. Results are presented here for the binary system *n*-formyl–Met–Phe (hereafter referred to as P) and *n*-formyl–Met–Trp (T). Feed solubility is an important factor, as for many other peptide mixtures, and its effect on the choice of solvent composition, feed retention, and resulting separations are discussed. It will be shown that the usual assumption of linear feed isotherms does not hold for the present system, due to the high feed concentrations generated at certain locations within the gradient schedule. In order to assess the effectiveness of these gradient runs, the same separations were done using nonlinear isocratic elution and stepwise elution.

2. Simulations

A lumped model of the chromatographic process [19,20] is used in the simulations. The mathematical formulation is as follows:

$$\frac{\partial c_i}{\partial t} + \nu_{\text{chrom}} \frac{\partial c_i}{\partial x} + \phi \frac{\partial q_i}{\partial t} = 0 \quad (1)$$

$$\frac{\partial q_i}{\partial t} = -k_{0,i}(q_i - q_i^*) \quad (2)$$

where t and x, the independent variables, are time and distance into the column respectively. The volumetric phase ratio is ϕ; ν_{chrom} is the chromatographic velocity; q_i is the adsorbed concentration of the i^{th} species, and q_i^* is the corresponding equilibrium value. The overall lumped rate coefficient k_0 can be related to the various physical sources of band spreading within the column-axial dispersion, film mass-transfer and pore diffusion — in a standard fashion for each component (e.g., [16]).

The form of the equilibrium expressions q^* to be used in Eq. (2) for P and T are derived from experiment as described below. The modulator is assumed to follow its own Langmuirian isotherm, but is unaffected by the feed components.

The entire coupled nonlinear hyperbolic system of partial differential equations is solved by the method of characteristics using a method that has been previously developed and applied to nonlinear isocratic elution, gradient elution with polymeric adsorbents, and displacement chromatography [16,21,22]. The initial and boundary conditions for the present problem represent a column that is initially free of any sample component (but pre-equilibrated to the relevant concentration of modulator), and sample introduction in the form of a finite pulse, followed by the introduction of the modulator gradient.

3. Experimental

3.1. Reagents

HPLC-grade acetonitrile (ACN) was obtained from EM Science (Gibson, NJ, USA), and sequanal-grade trifluoroacetic acid (TFA) from Pierce (Rockford, IL, USA). Water was distilled and deionized using the Megapure System (Coming, NY, USA). A mixture of monobasic and dibasic sodium phosphate from Mallinckrodt (Paris, KY, USA), adjusted to pH

7, was used as the buffer solution. All mobile phase components were degassed by helium sparging.

3.2. Apparatus

Preparative separations were carried out under ambient conditions at a flow-rate of 1 ml/min on a Waters (Milford, MA, USA) HPLC system consisting of a quaternary pump (Model 600), a UV detector (Model 486), and an autosampler (Model 717+) with a Novapak C_{18} column, 150 mm×3.9 mm I.D. The nominal particle size of the packing was 4 μm, with average pore size of 60 Å. The chromatograms, typically at a detection wavelength of 214 nm, were acquired on a DEC (Nashua, NH, USA) personal computer using Waters' MILLENNIUM software. Fractions were collected every 15 or 30 s for each preparative run, and analyzed (after dilution, if necessary) on another Novapak column with identical properties to the preparative column. Analytical runs were done isocratically at 20% ACN, using 20-μl samples at 1 ml/min under ambient conditions.

3.3. Measurement of retention factors and adsorption isotherms

The analytical retention factors of P and T were measured as a function of ACN concentration in a series of isocratic runs. The phase ratio was calculated from the column void volume, which was measured gravimetrically. The column was equilibrated with different mobile phases, MeOH–buffer (10:90, v/v) to MeOH–buffer (90:10, v/v). These data were used to fit a straight line, whose slope was proportional to V_0. The densities of the various mobile phases were taken from standard sources [23].

It is also necessary to assess the nonlinear adsorption behavior of the feed components. Here, single-component isotherms (SCIs) are measured by the method of elution by characteristic point (ECP): bands of each feed component are separately introduced into the column and eluted under isocratic conditions. The trailing edges of the resulting peaks are then used to calculate points on the single component isotherm of that feed component [24]. Since wide bands needed to be used in order to maximize the concentrations attained in the trailing bands, a slight modification of the standard method was necessary. The details of the method are given in Appendix A.

4. Result and discussion

4.1. Effect of feed state

The P+T mixture was found to have limited solubility at low ACN levels (10–15%), as will be discussed in detail in Section 4.2. Often, when solubility is limited, the feed mixture is dissolved in a liquid of different composition from that initially found in the column. However, such changes in the feed state were found to be unacceptable for this feed, as exemplified in Fig. 1. Panel (a) of Fig. 1 shows a gradient run from 10–40% ACN in 20 min, where the feed mixture of P+T is dissolved in the same state (ACN–buffer–TFA, 10:90:0.1, v/v) as is found initially in the column. The result is as expected, with the center of mass of the P peak around 15.5 min, and that of the T peak around 17 min. Both the feed peaks, as well as the impurity that emerges immediately after T, saturate the detector; nevertheless, a fairly good separation is seen. When the feed mixture is dissolved in ACN–buffer–TFA (40:60:0.1, v/v), while the initial state remains at ACN–buffer–TFA (10:90:0.1, v/v) and all other conditions are as in panel (a), a very different result is obtained (Fig. 1b). Some fraction of the feed moves along with the feed state and emerges just after the void volume; this is followed by a band that tails all the way back to a broad saturated peak. From analyses of fractions collected in such runs, it was found that both P and T are found throughout the peak near the void volume, and in the band that follows. It is clear that this is not a good separation.

Similar complications arise when the feed state is changed in other ways. For example, P is poorly soluble in the presence of TFA (see Section 4.2). When the feed state is kept at 10% ACN without TFA, a band that elutes close to the void volume is found again, but analysis of fractions showed that it contained only P. Nevertheless, the P was found to trail all the way into the T peak, giving a poor

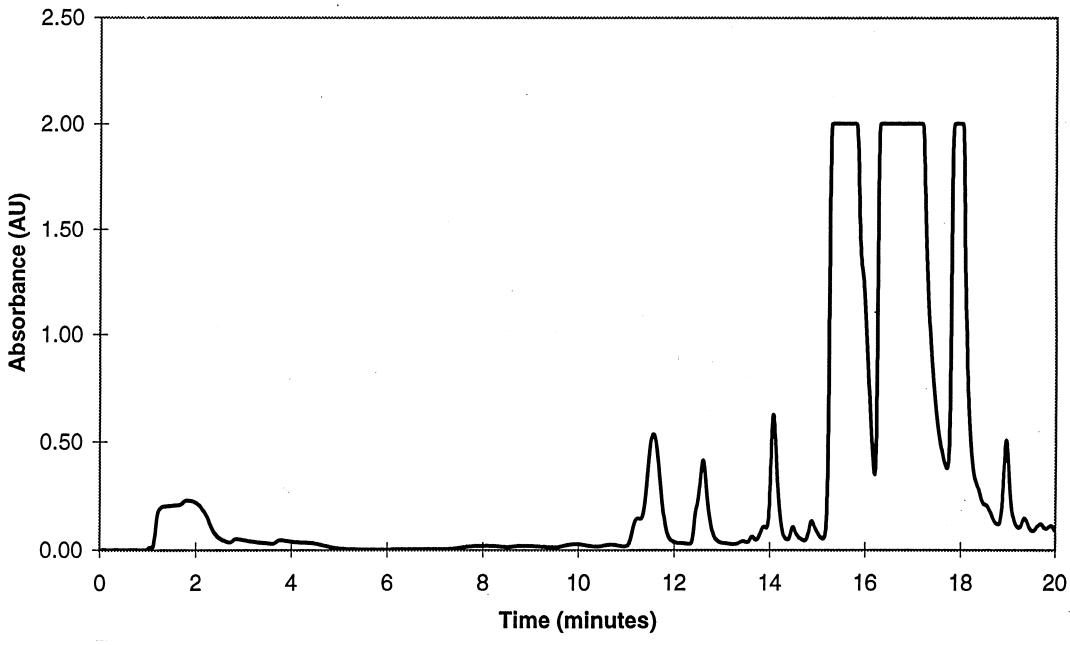

(a)

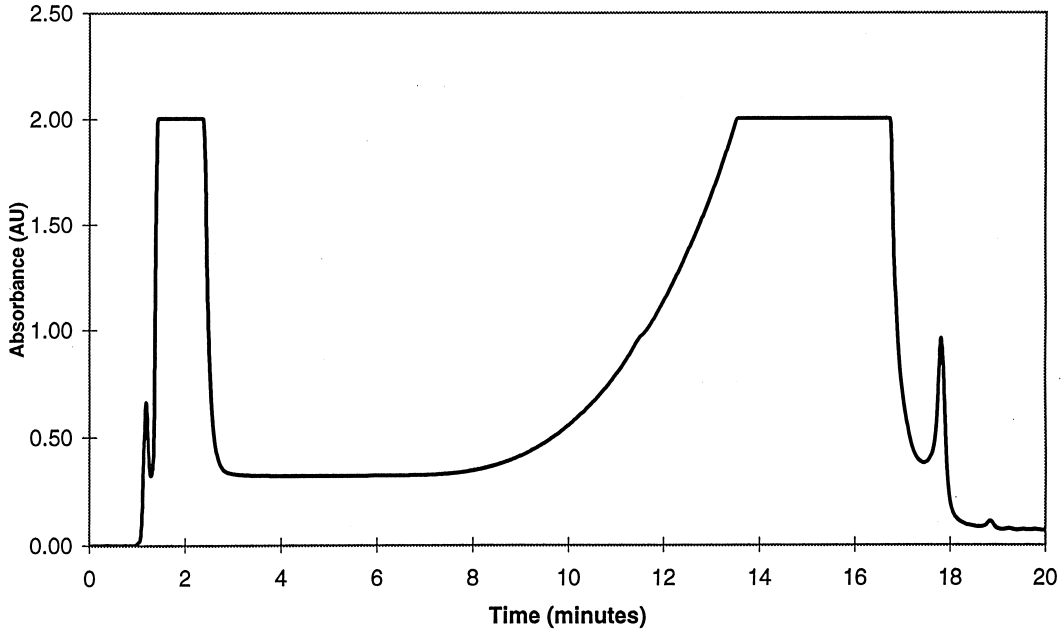

(b)

Fig. 1. Effect of feed state on separation quality. Panel (a) shows the UV trace of a gradient elution of P+T where the feed is dissolved in ACN–buffer–TFA (10:90:0.1, v/v) which is the initial state of the column. The gradient is 10–40% ACN in 20 min at a flow-rate of 1 mV/min; the feed is 0.5 mg/ml each of P and T in 1 ml feed volume; UV detection is at 214 nm at ambient temperature. Panel (b) uses a feed dissolved in ACN–buffer–TFA (40:60:0.1, v/v); other conditions as in panel (a).

separation. It therefore seems that for this system of P+T, it is necessary to keep the feed state identical to the initial state.

4.2. Solubility studies

First, we make some general observations. P is more soluble at neutral than at acidic pH, while T is fairly soluble at both neutral and acidic pH. Thus, at the low pH used in reversed-phase chromatography, the difficulty lies in solubilizing P. In addition, T is more soluble than P: in ACN–buffer (20:80, v/v) without TFA, 0.6 mg/ml P was soluble, but 1.0 mg/ml P was insoluble; 1.0 mg/ml T was soluble under the same conditions, as was the mixture of 1.0 mg/ml of P and T. In some cases, the presence of T seems actually to improve the solubility of P: in ACN–buffer (15:85, v/v) with 0.1% TFA added later (i.e., after the feeds have been added into the ACN–buffer solution), 0.75 mg/ml P was insoluble, but a mixture containing 0.75 mg/ml each of P and T was soluble.

In general, ACN–buffer solutions provided higher solubilities than the corresponding ACN–water solutions. For example, in the absence of TFA, 2.0 mg/ml of P alone was soluble in ACN–buffer (40:60, v/v), but insoluble in ACN–water (40:60, v/v). Again, with the immediate addition of 0.1% TFA (i.e., before the introduction of the feeds), ACN–buffer (10:90, v/v) could solubilize a mixture of 0.5 mg/ml each of P and T, but ACN–water (10:90, v/v) could not. Therefore, only ACN–buffer solutions will be considered in what follows.

Table 1 depicts solubility data for the P+T mixture, which is what is of practical interest. It can be seen that, in the absence of TFA, a mixture of 1.5 mg/ml each of P and T is soluble in ACN–buffer (40:60, v/v), but 1 mg/ml each is insoluble in 10:90 and even 0.5 mg/ml each is insoluble in 100% ACN. Thus the solubility of the P+T mixture is maximized at an intermediate level of ACN. More details about solubility of the P+T systems under a variety of other conditions can be found in the M.S. thesis of Kim [25].

The most important result in Table 1 from the point of view of subsequent separations is that the addition of TFA after the adsorbates have been put into the relevant ACN–buffer solutions seems to improve solubility, at least on the time scale of hours. For example, a mixture of 0.5 mg/ml each of P and T is insoluble in a solution of ACN–buffer–TFA (10:90:0.1, v/v), where all the solvent constituents are well mixed before the feeds are added (this is denoted by Prep. 1 in Table 2). But when 0.75 mg/ml each of P and T is put into a solution of ACN–buffer (10:90, v/v) and then 0.1% TFA is added, and the solution stirred for 30 min (this is Prep. 2 in Table 2), the adsorbates remain in solution. This is a metastable state, since continued stirring for several hours causes the solution to become cloudy. However, the time-scale of our separations is less than an hour, so we do not expect on-column precipitation to occur. The use of such metastable solutions appreciably increases feed concentrations. In all the runs that follow, 0.1% TFA is added after the feeds. The implications of possible interactions between P and T — suggested by the enhanced solubility of P in the presence of T — will be discussed later.

Table 1
Solubilities of P+T mixture as a function of mobile phase conditions

	1.0 P+T 10/90/0	1.5 P+T 40/60/0	0.5 P+T 100/0/0	0.75 P+T 20/80/0.1	1.0 P+T 40/60/0.1
Prep. 1	I	S	I	I	I
Prep. 2	N/A	N/A	N/A	S	S

The mobile phase is prepared in two ways: 'Prep. 1' in the table refers to the mixing of all mobile phase components (ACN, buffer, TFA) before the feeds are put in; 'Prep. 2' to the case where ACN and buffer are mixed, the feeds put into this mixture and stirred, and then the TFA is added.

Solubility is denoted by S, insolubility by I. In the column headings, the feed concentrations (in mg/ml) are given first, followed by the solvent specification in % (v/v), in the order ACN, buffer, TFA.

N/A=not applicable (because no TFA is used in these experiments).

Table 2
Feed retention factors as functions of ACN concentration

Component	A_1	B_1 (inverse v/v%)	A_2	B_2 (inverse v/v%)
P	1090	0.369	41.1	0.129
T	2220	0.401	66.5	0.140

Functional form in both cases is $k' = A_1 \exp(-B_1\varphi) + A_2 \exp(-B_2\varphi)$ where φ is the percentage volume fraction of acetonitrile in the mobile phase.

4.3. Retention factors and multicomponent isotherms

The retention factors of P and T as a function of ACN concentration are reported in Fig. 2. The data, shown as circles and squares, do not lie along straight lines in the semi-logarithmic plot, implying that retention factors do not decrease exponentially with modulator level, i.e., that these compounds are not 'linear solvent strength' adsorbates [1]. Since it is necessary to capture these data accurately for use in the simulations, they were fitted to a sum of 2 exponential terms, according to the equation

$$k' = A_1 \exp(-B_1\varphi) + A_2 \exp(-B_2\varphi) \quad (3)$$

The resulting fits are shown as solid lines in Fig. 2.

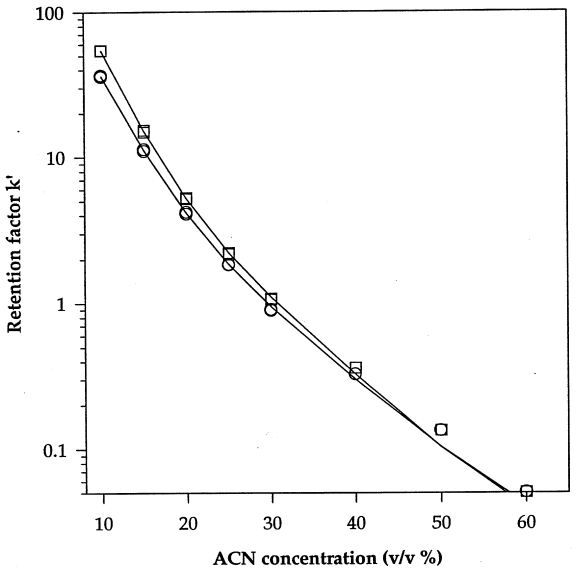

Fig. 2. Analytical retention factors of P and T as a function of ACN concentration. The data are shown as open circles (P) and open squares (T), and double-exponential fits to the data are shown as solid lines.

So both P and T have four parameters each in this fit. This is a large number of parameters, but it is necessary to fit the data in the experimental range accurately, so that simulations based on this fit can be rigorously tested against experiment. The fit is good for ACN levels below 40%, but worsens beyond that level. This divergence is unimportant here, because no experimental run exceeds 40% ACN. (In any case, the retention factors are very low beyond this level.) The relevant fitted parameters are listed in Table 2. It should be noted that the retention curves converge with increasing ACN, i.e., it might be expected that this would be a difficult separation for gradient elution.

The ECP method gave the SCIs shown in Fig. 3. An advantage of ECP is that several points on the

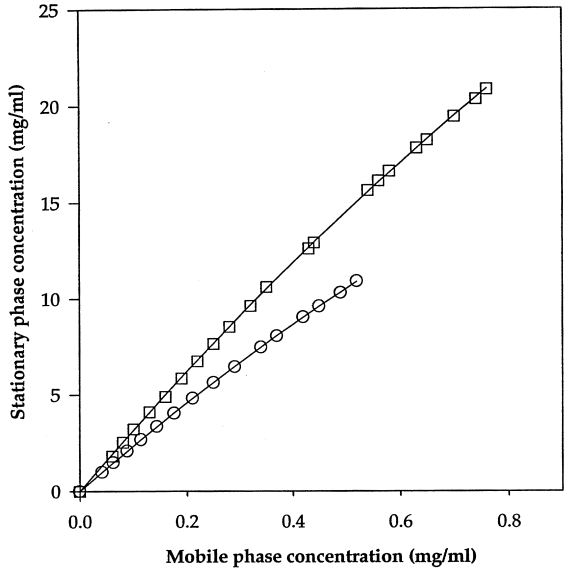

Fig. 3. Single-component adsorption isotherms for P and T. Measured by the elution-at-characteristic-point (FCP) method from several nonlinear isocratic runs for each component separately; all isocratic runs at ACB–buffer–TFA at ambient temperature.

SCI can be obtained from a single run. A disadvantage is that the bandspreading suffered by the trailing edge of the peak is assumed to be solely due to the nonlinearity of the SCI, i.e., the bandspreading caused by pore diffusion, film mass-transfer, etc. is neglected. To minimize this difficulty, data are taken from the higher portions of the trailing edges. The data in Fig. 3 seem to be linear, but they are limited by feed solubility (especially of P). At the much higher concentrations generated in the preparative runs (e.g., see Fig. 4), feed adsorption will definitely be nonlinear.

Classically, ECP is done using pure concentration overloading: high concentration plugs of very small volume are used [24]. Since our feeds have limited solubility, the ECP runs must use relatively large feed volumes, and consequently the effect of the feed volume must be accounted for. The correction is derived in Appendix A, and the generalized equation is given below:

$$q(c) = \int \frac{V(c) - V_0 - V_{\text{feed}}}{\phi V_0} \, \mathrm{d}c \tag{4}$$

where $V(c)$ is the eluting volume corresponding to any concentration c on the trailing edge of the peak. Correcting for the finite volume of the feed band merely introduces an additional V_{feed} term in the numerator of Eq. (4). When V_{feed} is small in relation to V_0, as is true for classical concentration overloading, V_{feed} can be dropped in the numerator, thus reducing Eq. (4) to the classical expression found in the literature (e.g., [24]). The data in Fig. 3 were fitted to the Langmuir isotherm, and these fits are shown as solid lines.

Multicomponent isotherms are more difficult to measure, especially for closely related compounds. Here, we make the approximation that the SCIs measured above can be combined in the usual way to generate multicomponent Langmuir isotherms. The Langmuir parameters will of course carry the double-exponential dependence on ACN concentration obtained earlier from the retention-factor runs. The general form of the multicomponent isotherms will therefore be:

$$q_{\text{P}} = \frac{\dfrac{k'_{\text{P}}}{\phi} c_{\text{P}}}{1 + \dfrac{k'_{\text{P}}}{\phi \Lambda_{\text{P}}} c_{\text{P}} + \dfrac{k'_{\text{T}}}{\phi \Lambda_{\text{T}}} c_{\text{T}}} \tag{5}$$

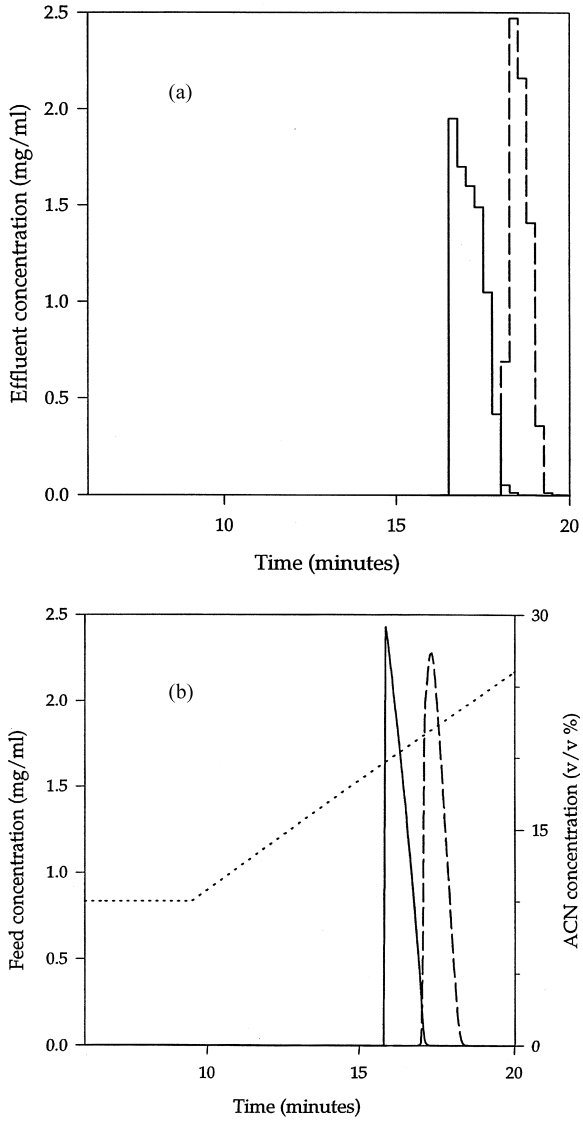

Fig. 4. Chromatogram of preparative gradient elution run; 0.71 mg/ml P and 0.68 mg/ml T in 2.4 ml feed volume containing 10% ACN. Gradient from 10–40% ACN in 20 min. Panel (a) shows the experimental result, and panel (b) the simulation using multicomponent feed isotherms. Ambient temperature; flow-rate 1 ml/min; fractions collected, diluted if necessary, and quantified (as described in the text) in order to construct the chromatogram. For the simulation, volumetric phase ratio $\phi = 0.46$; for ACN, Langmuir a parameter = 1.14 and Langmuir b parameter = 0.15 M^{-1} (from [10]).

and similarly for q_T. Here the Λ values are the saturation concentrations on the stationary phase; the other parameters are as described earlier. The retention factors are given by Eq. (3). The Λ values are estimated from the SCIs; since the solubility of P alone is so limited, its SCI is very slightly nonlinear, and therefore its Λ is poorly estimated.

Eq. (5) represents a multicomponent isotherm, i.e., self and mutual interference are accounted for. In the denominator of the right-hand side of Eq. (5), the second and third terms represent self and mutual interference, respectively. Thus dropping the third term would give only self interference, and dropping the second and third terms would remove both kinds of interference and therefore give the linear limit (classically used for feeds in gradient elution).

4.4. Preparative gradient runs

After the column was equilibrated at 10% ACN, gradients of 10–40% ACN in 20 min were carried out with 2.4 ml feed volume of the P+T mixture (itself at 10% ACN). Concentrations of about 0.7 mg/ml each of P and T were possible under these conditions. The UV trace at 214 nm for the preparative run showed complete saturation. Fractions were collected every 15 s, and reinjected (after dilution, if necessary) into the analytical column for analysis and quantification. Fig. 4a shows the result; it can be seen that the separation is extremely good, with near-quantitative recovery. Both feed peaks are extremely concentrated. Fig. 4b shows the analogous simulation, where the multicomponent isotherms given by Eq. (5) are used; reasonable agreement with experiment is found, given that there are no fitted parameters and the simulation is entirely predictive. The maximum concentration of P is somewhat overpredicted, and that of T somewhat underpredicted. However, the more important discrepancy is the underprediction of elution times. There are several possible reasons for this difference, such as accuracy of gradient formation, dwell time, and multicomponent isotherms [8].

Since a good separation was obtained at 2.4 ml, larger feed volumes were tried; Fig. 5 shows the corresponding run at 3 ml feed volume. Fig. 5a also shows the experimental results of collecting and analyzing 15-s fractions. The separation remains

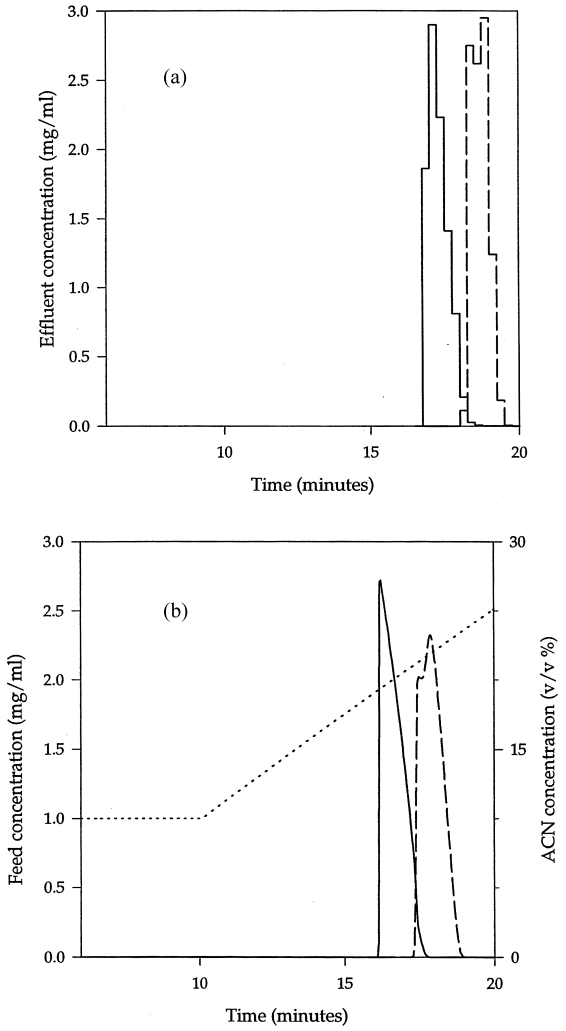

Fig. 5. Chromatogram of preparative gradient elution run; 0.73 mg/ml P and 0.72 mg/ml T in 3 ml feed volume containing 10% ACN. All other conditions as in Fig. 4.

near-quantitative, but P began to form crystals in several fractions, reflecting the extremely high concentrations reached. These fractions were redissolved by changing the pH to around 7. Thus, separations of this kind could be done by collecting the appropriate pool for P and immediately adding base to reach neutral pH, keeping the P in solution. Fig. 5b shows the corresponding simulation with multicomponent isotherms. Again, the maximum concentration of T is underpredicted.

To examine the effect of gradient slope, the

experiment in Fig. 4 was repeated with a shallower slope: a gradient of 10–30% ACN was run in 20 min. As expected, the focusing effect diminished as the gradient slope decreased, resulting in lower maximum concentrations. Smaller enrichment factors were obtained, as can be seen from the experimental run in Fig. 6a. The corresponding simulation in Fig. 6b captures the maximum concentrations of P and T quite well, but the elution times are appreciably underpredicted.

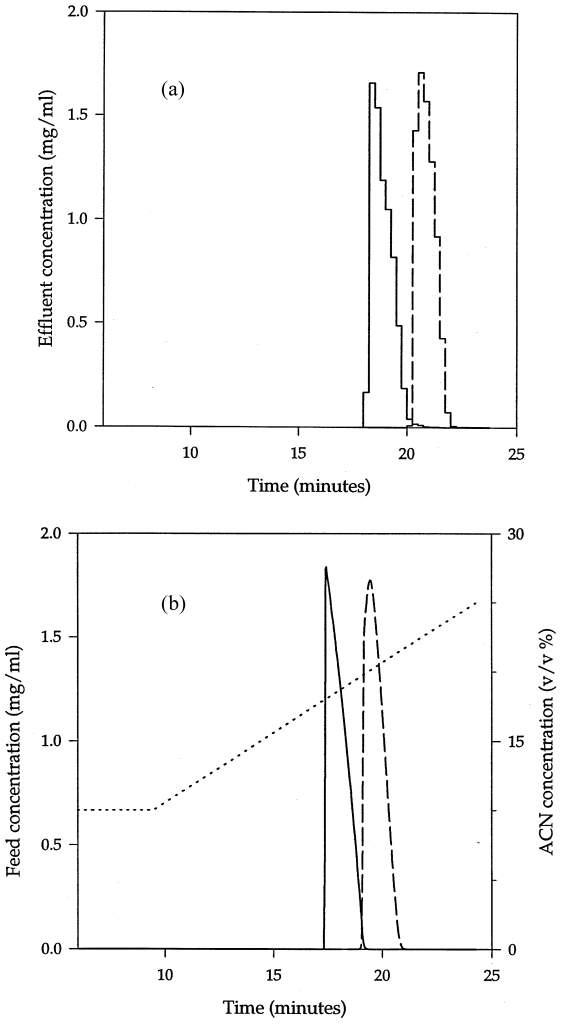

Fig. 6. Chromatogram of preparative gradient elution run; 0.75 mg/ml P and 0.75 mg/ml T in 2.4 ml feed volume containing 10% ACN. Gradient from 10–40% ACN in 30 min. All other conditions as in Fig. 4.

The solubility data showing that P is more soluble in the presence of T might seem to argue for secondary interactions between P and T. However, the regularity of peaks shapes in the foregoing runs (and in those that follow) imply that such secondary interactions — if they occur — do not impair separation quality.

4.5. Isocratic and stepwise elution runs

The same feed used in Fig. 4 was separated by nonlinear isocratic elution and stepwise elution, in order to compare these techniques quantitatively with gradient elution. Isocratic runs at 20% ACN gave considerable mixing even for a feed volume of 2.4 ml (chromatogram not shown). On the other hand, the retention factors in Fig. 2 make it clear that a run at 10% ACN will take an extremely long time. Thus, 15% ACN appeared to be a reasonable condition for nonlinear isocratic runs. In fact a good separation was achieved, as seen in Fig. 7. The corresponding simulation agrees well for P, but underpredicts the elution time for T. This is probably due to inaccuracies in the multicomponent isotherms, since they will have a greater effect for isocratic runs that for gradient runs (where gradient focusing plays an important role). The same run was repeated with a feed volume of 3 ml (chromatogram not shown), but appreciable mixing occurred, causing the yield to decrease. The corresponding productivity will be discussed later, when all the modes are compared.

The stepwise elution run used the following schedule: the column is initially at 10% ACN, as is the feed solution. The mobile phase composition is changed in a step from 10 to 15% ACN at 0.5 min (this step occurs at the gradient former, moves through the dead volume prior to the column and through the sample loop before reaching the column). Fig. 8 shows the result for a feed volume of 2.4 ml. The separation is almost quantitative, and — as in the isocratic case — the simulation describes P well and underpredicts the emergence of T by 2 min. This is to be expected, since after feed introduction, the feeds essentially move isocratically at 15% ACN. As in isocratic elution, small inaccuracies in the multicomponent isotherm can change the peaks appreciably. The separation quality is effectively unchanged upon increasing the feed volume to 3 ml,

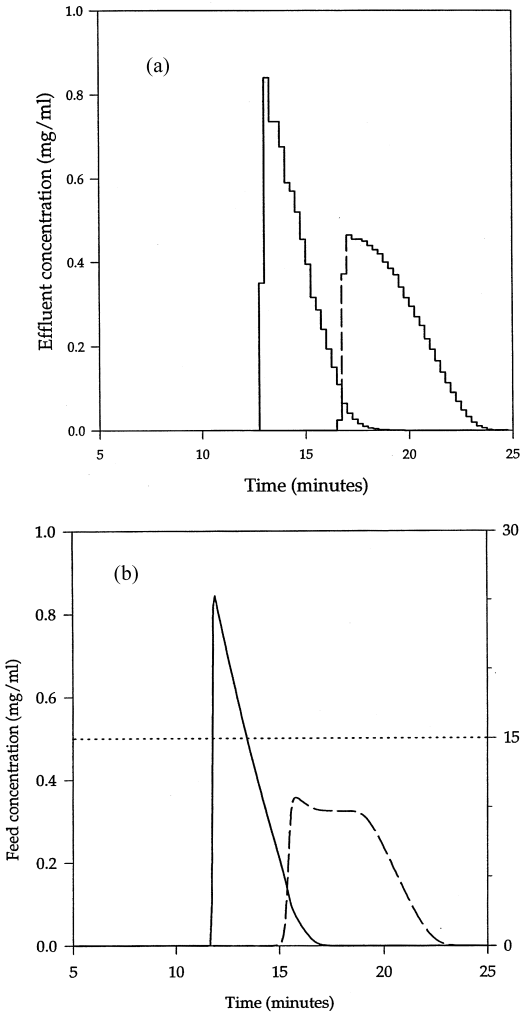

Fig. 7. Chromatogram of preparative nonlinear isocratic elution run at 15% ACN; 0.75 mg/ml P and 0.72 mg/ml T in 2.4 ml feed volume containing 15% ACN. All other conditions as in Fig. 4.

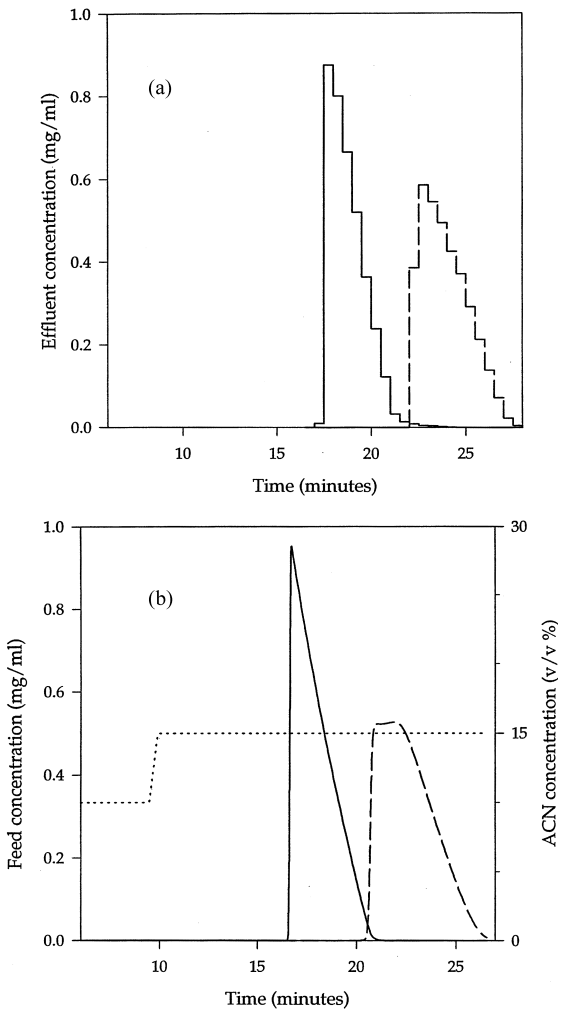

Fig. 8. Chromatogram of preparative stepwise elution run; 0.72 mg/ml P and 0.70 mg/ml T in 2.4 ml feed volume containing 10% ACN. The step from 10 to 15% ACN occurs at 0.5 min. All other conditions as in Fig. 4.

as shown in Fig. 9. Here the underprediction of the retention of T is reflected in more mixing in the simulation.

It should again be emphasized that, given the strongly nonlinear interactions involved in these runs, the predictive simulations show quite good overall agreement with experiments.

4.6. Efficacy of the operational modes

In order to compare the various runs quantitatively, we use the usual parameters relative to a specified product purity: production, defined as the amount of product recovered at the specified purity; yield, defined as the ratio of production to the amount in the feed stream; production rate, defined as the ratio of the production per unit mass of adsorbent to the cycle time. The cycle time includes not only the time of feed introduction and of separation, but also the regeneration time. These parameters are calculated for any run by computing the cut times satisfying the

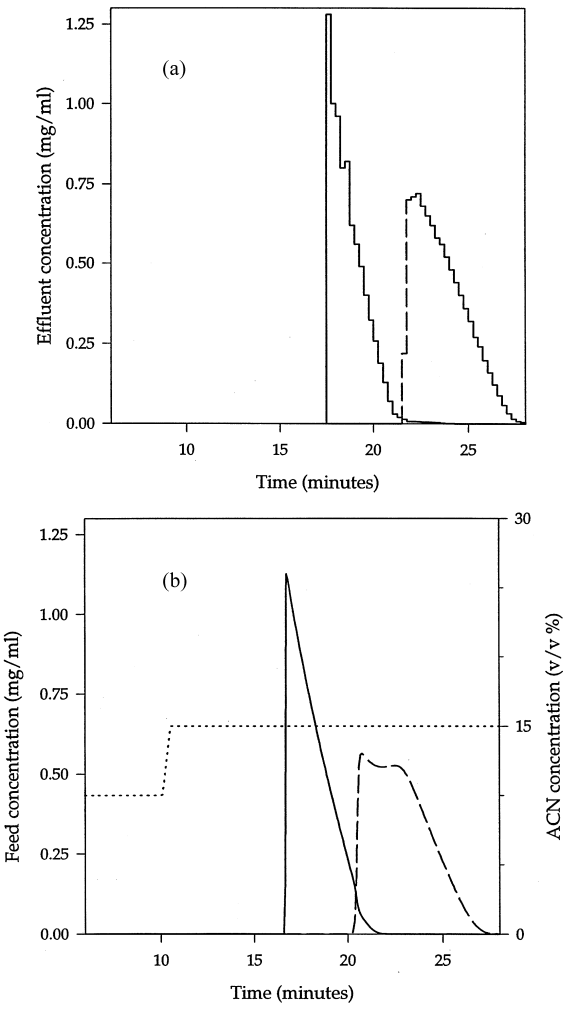

Fig. 9. Chromatogram of preparative stepwise elution run; 0.70 mg/ml P and 0.70 mg/ml T in 3 ml feed volume containing 10% ACN. All other conditions as in Fig. 8.

purity constraints: for each component, the cut times are chosen so that the average purity over the entire pool is equal to the specified amount. Then the other parameters can be easily calculated. Note that the cut times for each component are calculated assuming that it is the desired product; the cut times for P and T may therefore overlap. For all gradient and stepwise runs, a regeneration time of 20 min is added to each run. For the isocratic runs, a regeneration time of 10 min is used, corresponding to doing a wash step lasting 20 min to remove strongly bound material after every two runs, i.e., regeneration is assumed not to be needed after every run. The results are shown for a feed volume of 3 ml in Table 3.

It can be seen that there is not much to choose between the different methods. The higher production rate for isocratic compared to stepwise elution is due only to the lower regeneration time assigned to the former. The increased enrichment allowed by gradient elution is remarkable. Further, the maximum feed volumes for gradient elution were limited by solubility constraints. Simulations of even larger feed volumes (up to 5 ml) show that gradient elution continues to give extremely good separations, unlike the other techniques. The combination of the focusing power of the gradient with the multicomponent feed isotherms (that help to keep the feeds well separated at extremely high loadings) shows great promise for preparative separations.

4.7. Effect of feed interference and modulator adsorption

In order to assess the effect of feed interference,

Table 3
Comparison of the productivities, yields and enrichments of gradient, stepwise, and nonlinear isocratic elution runs

Type of elution	P			T		
	Productivity (mg/ml-h)	Yield (%)	Enrichment	Productivity (mg/ml-h)	Yield (%)	Enrichment
Isocratic	7.2	78	0.98	6.6	94	0.39
Stepwise	4.1	100	0.65	4.6	100	0.45
Gradient	6.1	100	2.1	6.4	100	2.3

Purity of 95% was required. In all cases, a feed volume of 3 ml was used. Enrichment is the ratio of the average concentration in the acceptably pure product to the feed concentration.

the run shown in Fig. 4 was simulated for the cases of no feed interference (linear feeds) and only self interference (noncompetitive feeds), as shown in Fig. 10. Fig. 10a shows the result for linear feeds; extremely high maximum concentrations of more than 6 mg/ml result for both P and T — obviously far higher than found in the experiment. (In fact, P would have precipitated on-column if it had reached these levels.) This is because, under linear feed isotherms, the peaks are controlled only by the focusing effect of the gradient, which would ideally cause the peaks to concentrate at a single point. This concentrating effect is countered by the bandspreading processes in the column, such as film mass transfer and pore diffusion, but these are not large for an efficient column. Thus the peaks become highly concentrated, and are consequently well separated. The peaks emerge later than those in Fig. 4a because linear feeds move more slowly than nonlinear ones (in fact, linear retention corresponds to the maximum retention, and the slowest chromatographic velocity, possible for that component). This result emphasizes the need to account for nonlinear feed adsorption, even in gradient elution. Fig. 10b shows the simulation for the case where self interference is allowed, i.e., each feed component competes with molecules of its own kind for binding sites on the adsorbent, but not with molecules of the other species. This somewhat artificial assumption nevertheless gives results that are much closer to the experiment in Fig. 4a than does the assumption of linear feeds. Because different concentrations move at different velocities under self interference, it becomes easier for the peak to counteract the focusing effect of the gradient to some extent. This broadens the peak somewhat, and dilutes it considerably. The peaks emerge faster than in Fig. 10a, but the lack of the displacement effect (mutual interference) leads to appreciable mixing between the peaks. By contrast, the separation in Fig. 4b, where both self and mutual interference are accounted for, allows the T to push the P ahead, improving the separation. Thus the real process can be conceptually regarded as twofold: gradient focusing localizes feed peaks, during which time interference may be neglected; then, when the peak concentrations become extremely high as a result of focusing, interference effects become important, diluting the peaks while simultaneously improving the separation.

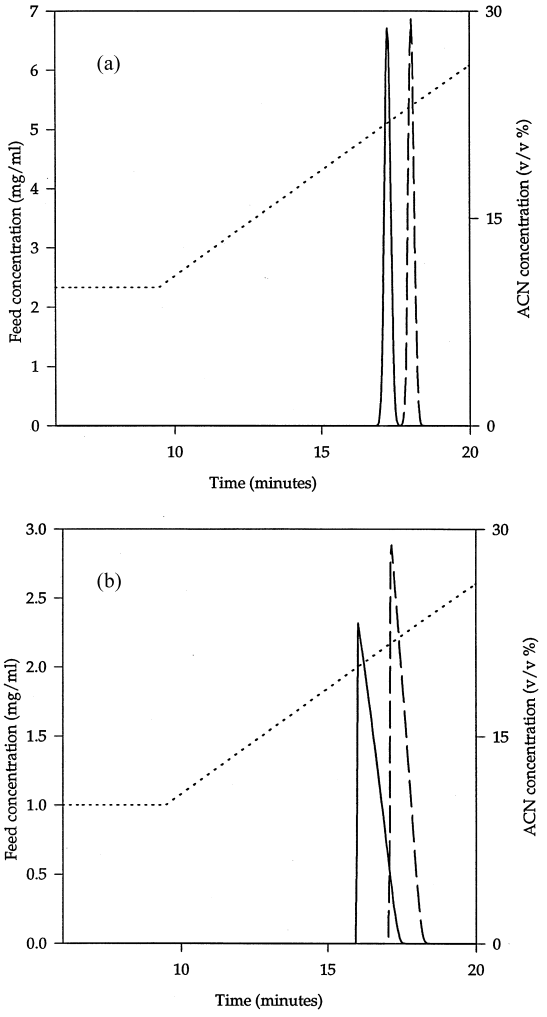

Fig. 10. Simulations of no and self-interference. The separation in Fig. 4 is simulated assuming no interference (linear feeds) in panel (a), and with only self-interference in panel (b).

The effect of accounting for the nonlinear adsorption of the acetonitrile modulator was also examined by simulation (chromatograms not shown). In all the cases shown above, the ACN is assumed to adsorb according to its own single-component Langmuir isotherm; since ACN retention is very similar on many silica-based C_{18} columns [26,27], the Langmuir parameters of El Fallah and Guiochon [10] were used. When ACN was assumed to be unretained, the gradient breaks through at 9.1 min, and when ACN is linearly retained, the gradient breaks

through at 9.7 min. The results for nonlinear ACN must lie between these two extremes [28], and in fact, the gradient breakthrough is at 9.5 min. These are small differences, and cause the feed peaks to change only by small amounts. Thus the effort of nonlinear modulator adsorption can be neglected here. But there are two cases where it must be accounted for. First, organic adsorption on polymeric reversed-phase adsorbents was found to be substantially larger than on silica-based reversed-phase adsorbents [16], and nonlinear adsorption must be accounted for on such polymeric sorbents. Second, even for silica-based sorbents, the extent of deviation caused by nonlinear modulator adsorption is proportional to the column length, and is likely to become quite important at preparative scale.

5. Conclusions

Preparative separations of chemotactic peptides by gradient elution have been carried out in reversed-phase chromatography. Large feed volumes (in relation to the column void volume) were used, at the maximum feed concentrations permitted by solubility, to achieve extremely good separations. Solubility is a complicated function of several parameters, including the presence of other feed components, and whether TFA was added before or after the feeds. Good solubilities were obtained in the latter case; although the situation appears to be metastable, the mixtures remain soluble for several hours, over which time a separation can be run, and the purified product put into a solution of neutral pH in which it is freely soluble. Quantitative separations were achieved for all the gradient elution runs, and the production rates seem to be limited only by solubility. The nonlinear isocratic and stepwise elution runs were also extremely good, but seem to have reached their maximum separating ability. Simulations using nonlinear feed isotherms agreed reasonably well with experiment, in marked contrast to the corresponding simulations with linear feed isotherms. Consequently, feed isotherms must be regarded as nonlinear in preparative gradient elution, contrary to the classical viewpoint. The combination of gradient focusing with multicomponent feed isotherms seems to be very useful for preparative separations. This is particularly significant in view of the low selectivity and the converging retention factor plots (Fig. 2), which argue for a difficult separation by gradient elution.

The separations here were not optimized, but the initial condition of 10% ACN was chosen to maximize the initial selectivity (see Fig. 2). Then a few values of gradient slope were used, and 10–40 ACN in 20 min was found to be the most effective of the slopes tried. So the results shown here cannot be used to conclusively determine the optimal gradient schedule; nevertheless, the convergence of the retention factors makes it unlikely that starting at significantly higher initial ACN values would be effective. Thus it seems probable that low initial modulator and relatively steep gradient slope are appropriate for this system, in order to maximize nonlinear interactions. A similar conclusion was reached by Jandera et al. [11] for the separation of phenol and *o*-cresol. However, further work is needed to elucidate optimal behavior for the general case.

Symbols

ACN	Acetonitrile
c	Mobile phase concentration of feed (mg/ml)
c_M	Mobile phase concentration of modulator (ACN), (M)
ECP	Elution by characteristic point
k'	Retention factor
k_0	Overall mass-transfer coefficient (m/s)
MCI	Multi-component (adsorption) isotherm
q	Stationary phase concentration (mg/ml)
q^*	Equilibrium stationary phase concentration (mg/ml)
SCI	Single-component (adsorption) isotherm
t	Time (min)
ν_{chrom}	Chromatographic velocity (m/s)
V_{feed}	Feed volume (ml)
V_0	Column void volume (ml)
x	Distance into column (m)

Greek symbols

ϕ	Volumetric phase ratio
φ	Modulator concentration %(v/v)

Appendix A

Here, the classical result for ECP is extended to account for finite feed volume. As shown in Fig. 11, the entire 'proportionate pattern' or trailing front of the peak emanates from the single point (0, t_{feed}), corresponding to the end of the feed injection pulse, t_{feed}. Therefore all points on this trailing edge enter the column at t_{feed}, and this time must be accounted for in the integrated equation for the chromatographic velocity. We begin with the classical equation [29] for ν_{chrom} under ideal chromatography:

$$\left(\frac{dx}{dt}\right)_c = \frac{\nu_{chrom}}{1 + \phi \frac{dq}{dc}} \tag{A1}$$

For a proportionate pattern, a given concentration moves with a velocity that remains constant throughout the run [30,31]. Hence, Eq. (A1) can be integrated, with 'initial' condition that $x=0$ at $t=t_{feed}$, according to the argument given above. The integration gives:

$$t(c) - t_{feed} = \frac{L}{\nu_{chrom}} \left(1 + \phi \frac{dq}{dc}\right) \tag{A2}$$

Noting that L/ν_{chrom} is t_0, and multiplying by the flow-rate so as to convert times into corresponding volumes, we get

$$V(c) - V_{feed} = V_0 \left(1 + \phi \frac{dq}{dc}\right) \tag{A3}$$

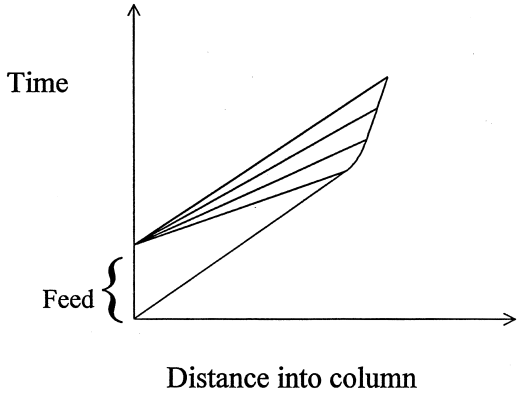

Fig. 11. Schematic distance–time diagram for ECP with nonnegligible feed volume.

from which the final result, Eq. (4) in the text, follows:

$$q(c) = \int \frac{V(c) - V_0 - V_{feed}}{\phi V_0} dc \tag{A4}$$

References

[1] L.R. Snyder, in Cs. Horváth (Editor), High-Performance Liquid Chromatography—Advances and Perspectives, Vol. 1, Academic Press, New York, 1980, pp. 208–316.
[2] P. Jandera, J. Churacek, Gradient Elution in Column Liquid Chromatography, Elsevier, Amsterdam, 1985.
[3] L.R Snyder, M.A. Stadalius, in Cs. Horváth (Editor), High–Performance Liquid Chromatography—Advances and Perspectives, Vol. 4, Academic Press: New York, 1986, pp. 195–312.
[4] S. Yamamoto, K. Nakanishi, R. Matsuro, Ion-Exchange Chromatography of Proteins, Marcel Dekker, New York, 1988.
[5] G. Guiochon, S. Golshan-Shirazi, A.M. Katti, Fundamentals of Preparative and Nonlinear Chromatography, Academic Press, New York, 1994.
[6] S.R. Gallant, S. Vunnum, S.M. Cramer, J. Chromatogr A 725 (1996) 295.
[7] F. Antia, Cs. Horváth, J. Chromatogr. 484 (1989) 1.
[8] M.Z. El Fallah, G. Guiochon, Biotechnol. Bioeng. 39 (1992) 877.
[9] M.Z. El Fallah, G. Guiochon, Anal. Chem.. 63 (1991) 859.
[10] M.Z. El Fallah, G. Guiochon, Anal. Chem. 63 (1991) 2244.
[11] P. Jandera, D. Komers, G. Guiochon, J Chromatogr. A 760 (1997) 25.
[12] D.D. Frey, Biotech. Bioeng. 35 (1990) 1055.
[13] H. Colin, J. Liquid Chromatogr. 11 (1988) 1809.
[14] S.J. Gibbs, E.N. Lightfoot, Ind. Eng. Chem. Fundam. 25 (1986) 490.
[15] A. Velayudhan, M.R. Ladisch, Chem. Eng. Sci. 47 (1992) 233.
[16] A. Velayudhan, R.L. Hendrickson, M.R. Ladisch, AlfChE J. 41 (1995) 1184.
[17] W.A. Marasco, S.H. Phan, H. Krutzsch, H.J. Showell, D.E. Feltner, R. Nairn, E.L. Becker, P.A. Ward, J. Biol. Chem. 259 (1984) 5430.
[18] E.O. Budrene, H.C. Berg, Nature 376 (1995) 49.
[19] D.M., Ruthven, Principles of Adsorption and Adsorptton Processes, Wiley, New York, 1984.
[20] R.T., Yang, Gas Separation by Adsorption Processes, Butterworths, Boston, 1987.
[21] A. Velayudhan, Ph.D. Dissertation, Yale University, New Haven, CT, 1990.
[22] A. Velayudhan, Cs. Horváth, Ind. Eng. Chem. Res. 34 (1995) 2789.
[23] R.H. Perry, D. Green, Perry's Chemical Engineers' Handbook, McGraw-Hill, New York, 1984.

[24] Conder, J.R., C.L. Young, Physico-Chemical Measurements by Gas Chromatography, Wiley, Chichester, 1979.
[25] B. Kim, M.S. Thesis, Oregon State University, Corvallis, OR, 1997.
[26] N. LeHa, J. Ungvaral, E. sz. Kováts, Anal. Chem. 54 (1982) 2410.
[27] K. Tani, Y. Suzuki, J. Chromatogr Sci. 27 (1989) 698.
[28] A. Velayudhan, M.R. Ladisch, in: T. Yoshida, R.D. Tanner (Editors), Bioproducts and Bioprocesses 2, Chapter 4.6, Springer-Verlag, Berlin, pp. 217–232.
[29] F. Helfferich, G. Klein, Theory of Multicomponent Chromatography, Marcel Dekker, New York, 1970.
[30] E. Glückauf, Disc. Faraday Soc. 7 (1949) 12.
[31] H.-K., Rhee, R. Aris, N.R. Amundson, First-Order Partial Differential Equations: Vol. I. Theory and Applications of Single Equations, Prentice-Hall, Englewood Cliffs, NJ, 1986.